NUCLEAR INSTRUMENTS AND METHODS 124 (1975) 477–484; © NORTH-HOLLAND PUBLISHING CO.

LINEAR FOCUSING OF NEUTRINO PARENTS

I. Elliptical Lenses

V. DOHM*, H. FAISSNER, F. J. HASERT, J. von KROGH and W. THOMÉ

III. Physikalisches Institut, Technische Hochschule Aachen, Aachen, Germany

Received 2 October 1974

This paper treats the general problem of focusing charged particles, e.g. neutrino parents, by means of (pulsed) rotationally symmetric current sheets. An exact parametric representation for the particle trajectories is given. The shape of a current sheet is derived which has ideal focusing properties for arbitrary angles. This shape is well approximated by an ellipsoid. The linearity of such an *elliptical lens* is demonstrated. This lens can be used to focus particles of a wide range of momenta. Elliptical lenses can be combined into lens systems, using the standard methods of geometrical optics.

1. Introduction

Neutrinos from high-energy meson decays travel very nearly in the original meson direction. Thus, an appreciable gain of intensity can be achieved by focusing the neutrino parents, which emerge from the target under rather large angles, on the neutrino detector. Since neutrino detectors are usually large and far away from the meson production target, the "ideal focusing" would be to bend all mesons parallel into a pencil beam. The corresponding increase in neutrino flux would be typically more than one order of magnitude. There is one serious difficulty: the generated mesons are not mono-energetic. Therefore, the focusing device must be very achromatic.

The first practical solution of this problem was given by van der Meer with his "magnetic horn" [1]). This device is essentially a double-walled funnel with a pulsed current flowing forth through, say, the inside conductor, and back through the outside one. A strong magnetic field is generated between the two conductors which bends particles of one sign of charge towards the horn axis, while defocusing those of the other sign. The target is inside the cylindrical section of the funnel. The horn has been run successfully during several stages of the CERN neutrino experiments, and it has increased the neutrino flux by about a factor of seven. Since then the original horn design[1]) has been improved considerably. Another substantial increase in neutrino flux was achieved by the addition of "magnetic reflectors" downstream from the horn[2]). Another focusing system has been developed by Palmer[3]); this, however, was especially tailored to the low-energy meson production spectrum. A magnetic horn of somewhat different construction was also successfully operated at ANL[4]).

In spite of these practical successes the operating principles of these devices remained somewhat obscure. Thus the shape of the CERN horn was modified several times empirically, in order to keep up with the improved knowledge of meson production spectra. Also it was soon recognized that the large conical part of the horn had very little effect as compared to the small cylindrical section enclosing the target. On the other hand, the effect of the conical section, and even more so that of the so-called reflectors[2]), resembled in some way the action of a field lens in geometrical optics.

It seemed desirable, therefore, to look for magnetic focusing devices with simple optical properties. The simplest device, of course, is a lens. It has the property to concentrate all impinging parallel rays into a point, or conversely, to render parallel all rays emerging from a point in the focal plane (fig. 1). One can easily construct a rotationally symmetric current sheet which for small angles has this property. The current generates a magnetic field outside the current sheet with a $1/y$-dependence, where y is the distance from the axis of

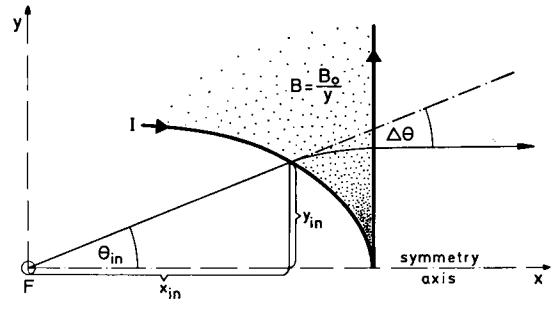

Fig. 1. Deflection of a charged particle in the magnetic field generated by a rotationally symmetric current sheet.

* Present address: Institut für Festkörperforschung der Kernforschungsanlage Jülich, Jülich, Germany.

symmetry. The condition that the device acts like a lens is the proportionality between the deflection angle $\Delta\theta$ and the y-coordinate of the entrance point (fig. 1):

$$\Delta\theta \propto y . \tag{1}$$

On the other hand, the deflection is given, in small-angle approximation, by the magnetic field $B(y)$ times the length x of the field seen:

$$\Delta\theta \propto B(y)\, x . \tag{2}$$

Since

$$B(y) = B_0\, y , \tag{3}$$

for all rotationally symmetric current sheets, the proportionality (1) of $\Delta\theta$ and y is obtained if

$$x \propto y^2 . \tag{4}$$

This simple consideration has already been made by Budker[5]). "Parabolic lenses" of this type have been built by his group[6]), and their use for neutrino-parent focusing has been discussed[7]). Clearly a technical advantage of this parabolic lens is its simplicity. On the other hand a drawback is its limitation to very small angles.

In the present paper we examine the focusing properties of rationally symmetric current sheets in detail. In particular we derive and discuss the general shape of a current sheet, which focuses exactly for arbitrary angles. To a high degree of accuracy this shape can be approximated by a simple contour: an ellipsoid.

2. Motion of a charged particle in a $1/y$-field

Let us consider the motion of a charged particle in a magnetic field B generated by a rotationally symmetric current I. The magnetic field lines outside the current sheet are circles around the symmetry axis (x-axis, see fig. 1). Inside the sheet the field is zero. Since the particle's momentum component parallel to the field lines is not influenced by the field it is sufficient to discuss the motion in an arbitrary plane containing the x-axis. Our aim is to derive and solve the differential equation for the trajectory of the particle in this plane (the x–y-plane).

The field strength (in rationalized mKs units) is given by:

$$B(y) = \frac{\mu_0}{2\pi}\frac{I}{y} . \tag{5}$$

At any given point the Lorentz force due to the local magnetic field $B(y)$ determines the radius of curvature ρ of the trajectory according to

$$\rho = \frac{p_0}{q}\frac{1}{B} , \tag{6}$$

where p_0 and q are the momentum and charge of the particle, respectively.

The line element $\mathrm{d}s$ of the trajectory is given by (fig. 2)

$$\mathrm{d}s = -\rho\,\mathrm{d}\Theta . \tag{7}$$

In addition we have the geometric relations

$$\mathrm{d}y = \sin\Theta\ \mathrm{d}s , \tag{8}$$

$$\mathrm{d}x = \cos\Theta\ \mathrm{d}s , \tag{9}$$

where Θ is the angle between the x-axis and the tangent of the trajectory at the given point. Substituting eq. (7) into eqs. (8) and (9), and using eqs. (6) and (5), we obtain two coupled differential equations:

$$\frac{\mathrm{d}y}{y} = -A_0 \sin\Theta\ \mathrm{d}\Theta , \tag{10}$$

$$\mathrm{d}x = -A_0\, y \cos\Theta\ \mathrm{d}\Theta , \tag{11}$$

with

$$A_0 = \frac{2\pi}{\mu_0 q}\frac{p_0}{I} . \tag{12}$$

For a given initial condition $y_{\mathrm{in}} = y(\Theta_{\mathrm{in}})$, the integration of eq. (10) yields:

$$y = y_{\mathrm{in}} \exp\{A_0(\cos\Theta - \cos\Theta_{\mathrm{in}})\} . \tag{13}$$

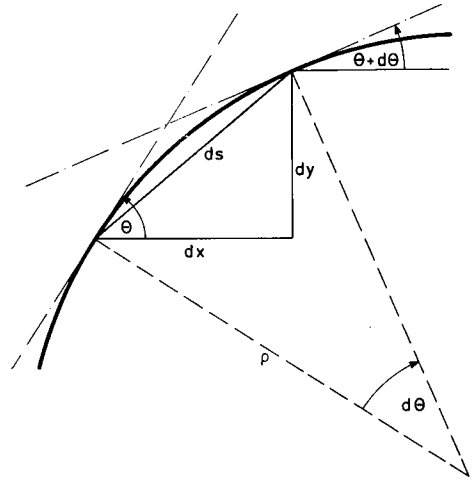

Fig. 2. The line element of a particle trajectory at an arbitrary point in the magnetic field.

Inserting this into eq. (11) we find:

$$x - x_{in} = A_0\, y_{in} \times \times \int_{\Theta}^{\Theta_{in}} d\theta \cos\theta \exp\{A_0(\cos\theta - \cos\Theta_{in})\}, \tag{14}$$

with $x_{in} = x(\Theta_{in})$. Thus, with eqs. (13) and (14), we have the exact parametric representation $y(\Theta)$, $x(\Theta)$ for a trajectory which starts from the point y_{in}, x_{in} with an angle Θ_{in}.

3. Elliptical current sheet

We use the solution (13), (14) to derive the shape of a current sheet with lens properties. Again we treat this problem in the x–y-plane; the actual lens is obtained by rotation around the symmetry axis. For the sake of convenience we consider a "plano-convex" lens (fig. 1), i.e. we terminate the field region by the plane

$$x = f_0 = \text{constant}, \qquad y = \text{arbitrary}.$$

A lens makes all trajectories parallel to the axis which emerge, under arbitrary angles Θ_{in}, from the focal point F. Thus

$$\Theta_{out} = 0.$$

This, inserted into eq. (14), yields the desired relation for the *initial boundary of the field region*, namely the shape of the lens:

$$f_0 - x_{in} = A_0\, y_{in} \times \times \int_{0}^{\Theta_{in}} d\theta \cos\theta \exp\{A_0(\cos\theta - \cos\Theta_{in})\}. \tag{15}$$

Conversely, this lens focuses exactly particles with uniform momentum $p_0 (\mu_0 = q/2\pi)\, A_0 I$, entering the lens parallel to the axis, from the opposite direction. Note that in eq. (15) the entrance angle Θ_{in} is a function of x_{in} and y_{in} according to:

$$\tan\Theta_{in} = y_{in}/x_{in}. \tag{16}$$

So far no approximations have been used. Since we are interested in relatively small entrance angles only, we expand the cosine and the exponential function in eq. (15), and require:

$$\Theta_{in}^2 \ll 1, \tag{17}$$

$$A_0^2 \Theta_{in}^4 \ll 1. \tag{18}$$

Keeping only the leading terms we obtain from eqs. (15) and (16) (see appendix A):

$$\frac{f_0 - x_{in}}{f_0}\left(1 - \frac{4}{3}\frac{f_0 - x_{in}}{f_0}\right) = A_0 \left(\frac{y_{in}}{f_0}\right)^2. \tag{19}$$

This can be rewritten as:

$$(x_{in} - \tfrac{5}{8} f_0)^2 + \tfrac{3}{4} A_0\, y_{in}^2 = (\tfrac{3}{8} f_0)^2, \tag{20}$$

which is the equation of an ellipse. Major and minor half-axis are given by

$$a = \tfrac{3}{8} f_0, \qquad b = 2a/(3A_0)^{\frac{1}{2}}, \tag{21}$$

and the ellipse parameter is

$$h = b^2/a = f_0/2A_0. \tag{22}$$

Thus we have arrived at the simple result that the desired current sheet is approximately an ellipsoid.

The connection with the parabolic lens mentioned in the introduction is easily established by using the small-angle approximation more restrictively. Instead of eq. (18) we require:

$$A_0 \Theta_{in}^2 \ll 1. \tag{23}$$

Eq. (19) then reduces to:

$$2h(f_0 - x_{in}) = y_{in}^2, \tag{24}$$

with

$$h = f_0/2A_0. \tag{25}$$

Thus the parabolic lens[5, 6]) is obtained. In either case the focal length f_0 is fixed, for constant A_0, by the ellipse (or parabola) parameter h.

4. Optical properties: angular dependence

In this section we study the quality of the approximation used in obtaining the ellipsoid. We discuss the angular dependence of its focusing properties, in particular with respect to linearity.

By construction, the current sheet described by eq. (15), with A_0 and f_0 fixed, focuses exactly a particle of a well defined momentum

$$p_0 = (\mu_0 q/2\pi)\, A_0 I, \tag{26}$$

where I is the current flowing through the sheet. This holds for all entrance angles. We have calculated the exact lens shape by integrating eq. (15) numerically. In fig. 3 the elliptical lens is compared with this exact shape as well as with the parabolic lens for a realistic value of A_0.

The exact lens is well reproduced by the ellipsoid up to angles of 35 mrad whereas the parabolic lens

deviates significantly from the true shape above 8 mrad. This demonstrates the superior focusing properties of the elliptical lens, which are even more pronounced for larger values of A_0. This limiting angle of 35 mrad corresponds to a transverse momentum of 350 MeV/c for a total momentum of 10 GeV/c. In nucleon–nucleon interactions the transverse momenta of the secondary mesons are of the same order. Thus elliptical lenses should be well suited for use as focusing elements in a high-energy neutrino beam.

Another feature, which makes the elliptical lens even more attractive, is the fact that ideal focusing implies ideal linearity provided that $\Theta_{in} \ll 1$. Then we have:

$$|\Delta\Theta| \equiv |\Theta_{out} - \Theta_{in}| = |\Theta_{in}| = \frac{1}{f_0}|y_{in}|, \qquad (27)$$

since $\Theta_{out} = 0$ (ideal focusing). This is just the condition for linearity as given by eq. (1). Thus the elliptical lens is linear and focuses ideally in the angular range limited by eq. (18).

The linearity of the elliptical and parabolic lens is illustrated in fig. 4. The above discussion refers to the set of curves with $p = 20$ GeV/c (for a complete discussion of fig. 4, see the next section). The superiority of the elliptical lens (full line) as compared to the parabolic lens (dotted line) is striking.

5. Optical properties: momentum dependence

So far the discussion refers to particles of a single momentum p_0 only. In actual applications, however, we have to deal with a wide range of momenta. Therefore, it is necessary to examine the momentum dependence of the lens properties. For simplicity, we confine the discussion to the case of the parabola. The results also apply to the ellipsoid, at least qualitatively.

We consider the parabolic lens given by eq. (24) with h and I fixed, traversed by a particle with *arbitrary* momentum p. For given initial parameters Θ_{in}, x_{in}, y_{in}, the exit angle Θ_{out} of the trajectory at $x = f_0$ is determined by eq. (14):

$$f_0 - x_{in} = A\, y_{in} \times \int_{\Theta_{out}}^{\Theta_{in}} d\theta \cos\theta \exp\{A(\cos\theta - \cos\Theta_{in})\}, \qquad (28)$$

with

$$A = \frac{2}{\mu_0 q I} p, \qquad p \text{ variable}. \qquad (29)$$

This equation depends upon the distances only through the ratios x_{in}/f_0 and y_{in}/f_0. Thus a change in design momentum p_0, by a factor of K, leads to the same trajectories, if the distances are scaled up by the factor K too. None such simple scaling law holds if, at fixed p_0, the particle momentum p varies. But in small-angle approximation the effect of p is readily assessed:

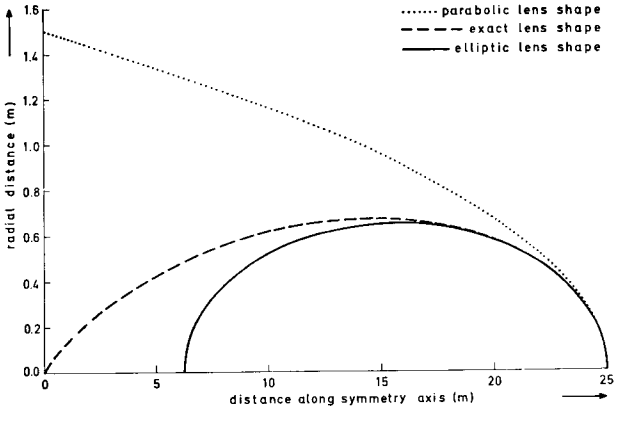

Fig. 3. Comparison of the elliptical and parabolical lens with the exact lens. For the calculation the following parameters were used: $f_0 = 25$ m, $I/p_0 = 60$ kA(GeV/c)$^{-1}$, corresponding to $A_0 = 278$.

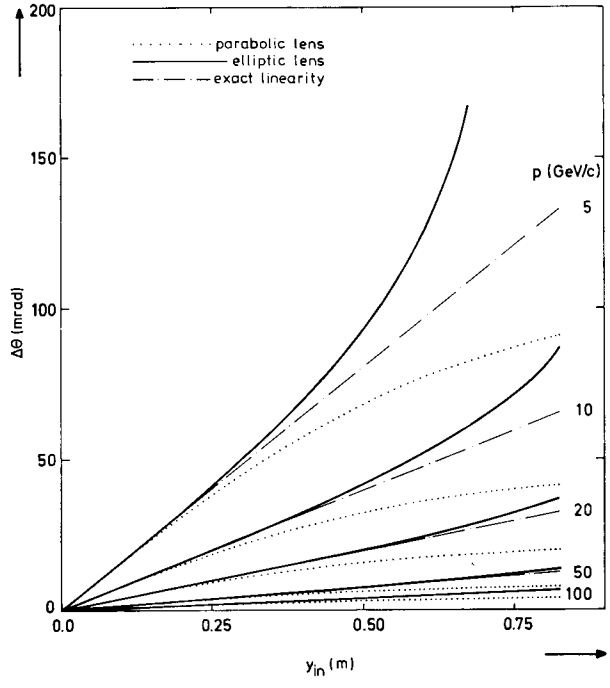

Fig. 4. Momentum dependence of linearity – comparison of elliptical and parabolic lens. For this calculation the following parameters have been used: $f_0 = 25$ m, $I/p_0 = 30$ kA(GeV/c)$^{-1}$, corresponding to $A_0 = 555$.

If one requires:

$$\Theta_{\text{out}}^2 \ll 1, \tag{30}$$

and employs again the parabolic approximation:

$$A\Theta_{\text{in}}^2 \ll 1, \qquad A\Theta_{\text{out}}^2 \ll 1, \tag{31}$$

eq. (28) reduces to:

$$f_0 - x_{\text{in}} = (\Theta_{\text{in}} - \Theta_{\text{out}})\, A y_{\text{in}}. \tag{32}$$

Inserting eq. (24) into eq. (32) we obtain linearity:

$$\Theta_{\text{in}} - \Theta_{\text{out}} = \frac{A_0}{f_0 A}\, y_{\text{in}}. \tag{33}$$

Here Θ_{out} need not be zero.

In appendix B we show that the range of momenta p for which linearity holds is limited by:

$$\left(\frac{p-p_0}{p}\right)^2 \Theta_{\text{in}}^2 \ll 1, \tag{34}$$

where p_0 is given by eq. (26). For $p \gtrsim p_0$ the necessary condition (34) is automatically fulfilled according to eq. (17). Thus, the significance of eq. (34) is to give a lower bound for p (if Θ_{in} is given) or, alternatively, an upper bound for Θ_{in} (if $p < p_0$ is given):

$$\Theta_{\text{in}}^2 \ll \frac{p^2}{(p_0-p)^2}. \tag{35}$$

The momentum dependence of linearity is illustrated in fig. 4. We mention two points:

1) The qualitative behaviour for the paraboloid and the ellipsoid is the same: the deviation from linearity increases with decreasing momentum p, in agreement with eq. (34).
2) For the ellipsoid linearity extends to considerably higher entrance angles than for the paraboloid, for arbitrary momenta.

We expect that not only better linearity but also better focusing holds for the ellipsoid in the momentum range considered above. For values of p around p_0 this is certainly true as discussed in section 4.

So far, the particle source has been assumed to be located at a distance f_0 from the lens plane, independent of the momentum p. An adjustment of this distance for arbitrary p is desirable. For this reason we introduce appropriate – momentum-dependent – quantities: the focal length $f(p)$ and the focusing function $F(p)$.

They are defined, respectively, by:

$$\Theta_{\text{in}} - \Theta_{\text{out}} = \frac{1}{f(p)}\, y_{\text{in}}, \tag{36}$$

and

$$F(p) = \Theta_{\text{out}}/\Theta_{\text{in}}. \tag{37}$$

From eq. (33) we obtain:

$$f(p) = \frac{4\pi h}{\mu_0 q I_0}\, p. \tag{38}$$

Of course,

$$f(p_0) = f_0.$$

For the focusing function, eq. (36) yields:

$$F(p) = 1 - \frac{d}{f(p)}, \tag{39}$$

where the length:

$$d = y_{\text{in}}/\Theta_{\text{in}}$$

is the distance between the particle source and the lens plane.

For actual applications, this distance can be suitably chosen: If $d = f(p)$, $F(p) = 0$, which means perfect focusing; for $|F(p)| < 1$ some focusing is achieved. $F(p) < 0$ means that the slope of the particle's trajectory has changed sign.

6. Numerical illustrations

This section serves to illustrate the action of an elliptical lens on a beam of particles with a wide range of momenta. This was done by tracing a given particle through the magnetic field step by step. The exact particle trajectory was obtained by numerical integration of the differential equation (14) on a computer.

For this computation the following lens parameters were chosen: $f_0 = 25$ m and $I/p_0 = 30$ kA(GeV/c)$^{-1}$, corresponding to $A_0 = 555$. The lens was pulsed with a current of $I = 600$ kA, and the distance between particle source and the lens was taken as 50 m. From the discussion in section 5 we expect particles with a momentum of $p = 40$ GeV/c to be focused exactly at this distance. As input a "white" beam of particles was chosen, i.e. the particles were assumed to be equally distributed over momenta between 5 and 150 GeV/c and angles between 0 and 5 mrad. This flat distribution became slightly distorted by the finite acceptance of the lens, since particles which did not pass through the lens were rejected.

The action of the lens on this beam of particles is demonstrated in fig. 5, which shows the output spectrum as a function of both momentum and angular divergence. There is a pronounced peak of parallel

particles at a momentum of 40 GeV/c, as expected from our general discussion. At higher momenta there is still some focusing action; low momenta, of course, are strongly overfocused.

7. Discussion

This paper treated the general problem of focusing charged particles by rotationally symmetric current sheets. The central idea was to achieve linear focusing, i.e. to obtain a lens. This problem was solved exactly. As the numerical calculations confirmed, the resulting tadpole-shaped current sheet showed linear focusing at arbitrary angles. A very useful approximation to this exact shape turned out to be, for small emission angles, an ellipsoid. Restricting the emission angle even further leads to the paraboloid of Budker's[5]). The properties of these three lens types have been verified by extended calculations. For focusing neutrino parents at 30 or 300 GeV elliptical lenses seem to be adequate.

Of course, a single lens, whether ideal or not, is not very suited to focus the broad spectrum of mesons produced by high-energy protons. But the solution to this problem is obvious: one has to use *lens systems*. Such systems can be readily composed of linear lenses,

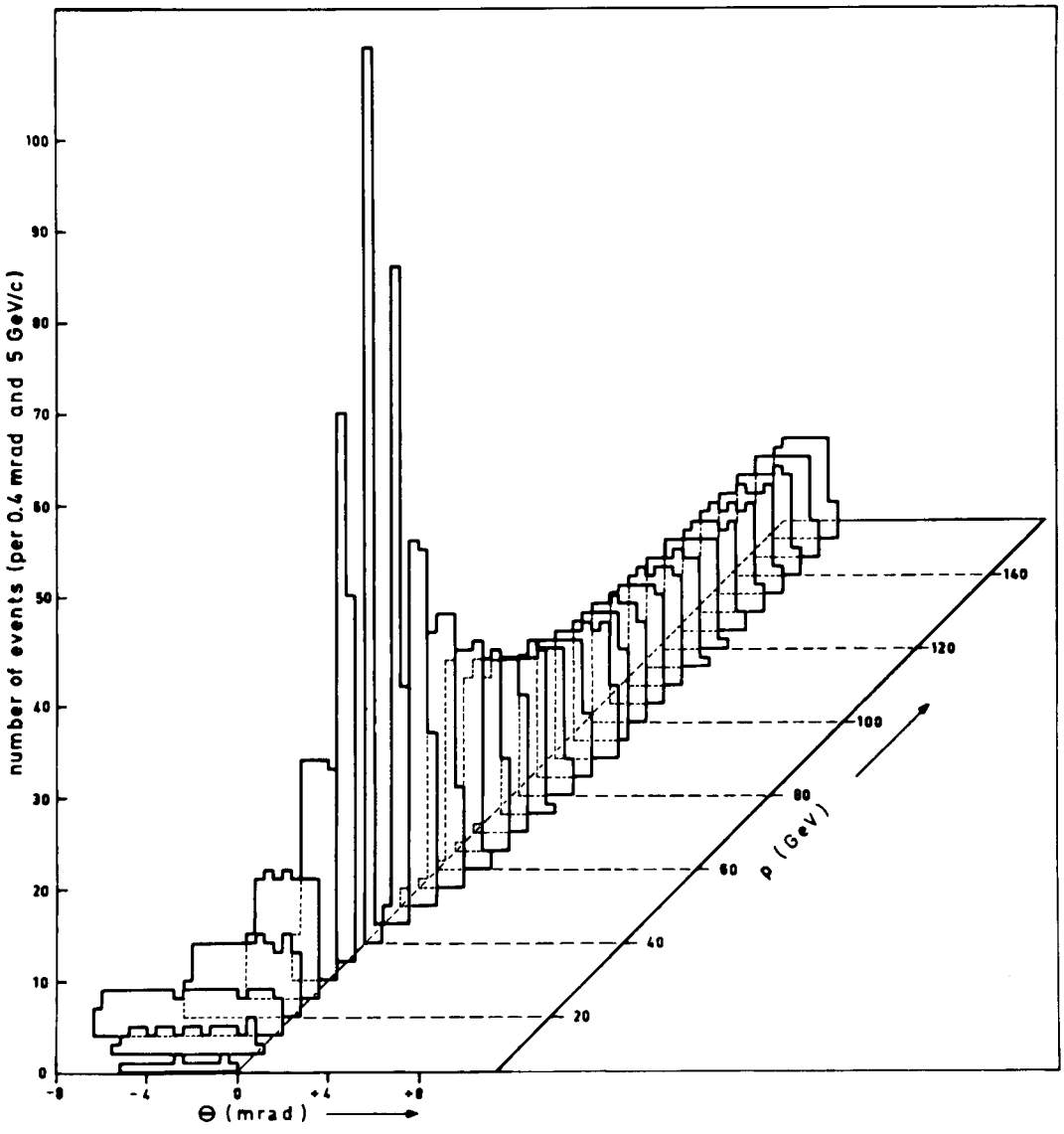

Fig. 5. Angular and momentum output spectrum illustrating the action of an elliptical lens. As input the particles were assumed to be equally distributed over momenta between 5 and 150 GeV/c and angles between 0 and 5 mrad.

and their properties can be easily computed from the properties of their components. The standard matrix methods of geometrical optics are most suitable for this purpose. This has been emphasized already by the Russian group[7]). A related advantage of these lens systems is their flexibility: by some change in distances and currents their optical properties can be drastically altered. Thus it is conceivable that the same elliptical lenses provide, according to wish, a high-intensity wide-band neutrino beam, a medium-band beam, or a high-pass beam. These questions have been touched upon in our previous report[9]). They will be treated more in full in our forthcoming 2nd part.

Yet all these considerations are somewhat academic. For the actual construction of lenses practical points of view come into play. When focusing neutrino parents one wants as little as possible material in the way of the particles. This clearly runs against the requirements of mechanical stability under the severe stresses induced by the high currents. Yet, as indicated in fig. 6, the elliptical shape has one advantage: Far away from the axis, where the particles enter under small angles to the surface, the stresses are small and the conductor can be made thin. On the other hand, near axis, where the fields and forces are enormous, and where a thick layer is a necessity, the particles cross almost normal to the surface. The Budker group has already gained experience in these questions[6]).

Finally, one will have to consider, whether one would like to stick accurately to the exact or elliptical shape. It might be impedient, instead, to approximate them crudely by simple shapes, like cylinders and cones. Admittedly, one would lose in clarity of the mathematical treatment. But one might gain in ease of fabrication. We hope to come back to these questions in a future report.

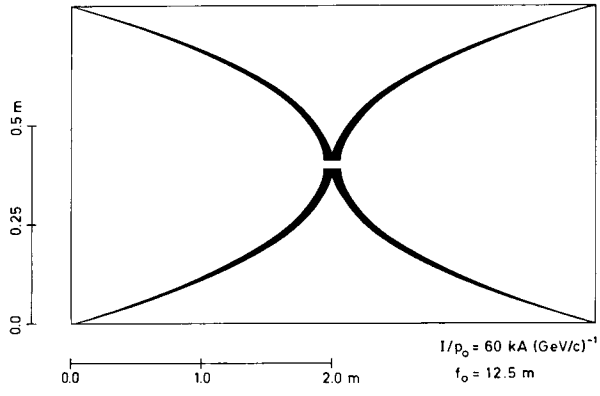

Fig. 6. Elliptical double lens with half the focal length of a single lens. Varying wall thickness is indicated.

Some of the authors enjoyed useful discussions with Drs A. Ašner, S. van der Meer, and R. B. Palmer. The senior author (H. F.) wants to thank Prof. G. I. Budker for bringing the Russian work to his attention. Finally, the authors are grateful to Mme Chantal Koenig for her patient and diligent typing of the various versions of the manuscript.

Appendix A

Elliptical approximation

For

$$\tfrac{1}{2}\Theta_{in}^2 \ll 1 \tag{40}$$

eq. (15) becomes:

$$f_0 - x_{in} = A_0\, y_{in} \times \times \int_0^{\Theta_{in}} d\theta \exp\{\tfrac{1}{2} A_0(\Theta_{in}^2 - \theta^2)\}. \tag{41}$$

Furthermore, in the "elliptical approximation",

$$\tfrac{1}{8} A_0^2 \Theta_{in}^4 \ll 1, \tag{42}$$

the exponential function in eq. (41) can be replaced by

$$1 + \tfrac{1}{2} A_0(\Theta_{in}^2 - \theta^2).$$

Then the integration yields:

$$f_0 - x_{in} = A_0 y_{in}\, \Theta_{in}(1 + \tfrac{1}{3} A_0 \Theta_{in}^2), \tag{43}$$

or:

$$\frac{f_0 - x_{in}}{x_{in}} = A_0 \left(\frac{y_{in}}{x_{in}}\right)^2 + \tfrac{1}{3} A_0^2 \left(\frac{y_{in}}{x_{in}}\right)^4, \tag{44}$$

because of $\Theta_{in} = y_{in}/x_{in}$. In the same approximation, eq. (44) may be rewritten as:

$$\frac{f_0 - x_{in}}{x_{in}} = A_0 \left(\frac{y_{in}}{x_{in}}\right)^2 + \frac{1}{3}\left(\frac{f_0 - x_{in}}{x_{in}}\right)^2,$$

or:

$$\frac{f_0 - x_{in}}{f_0}\,\frac{x_{in}}{f_0} = A_0 \left(\frac{y_{in}}{f_0}\right)^2 + \frac{1}{3}\left(\frac{f_0 - x_{in}}{f_0}\right)^2. \tag{45}$$

Inserting:

$$\frac{x_{in}}{f_0} \equiv 1 - \frac{f_0 - x_{in}}{f_0},$$

we finally have:

$$\frac{f_0 - x_{in}}{f_0}\left(1 - \frac{4}{3}\frac{f_0 - x_{in}}{f_0}\right) = A\left(\frac{y_{in}}{f_0}\right)^2. \tag{46}$$

This is eq. (19) of the elliptical current sheet discussed in the text.

Appendix B

Parabolic approximation

In the "parabolic approximation" (23),

$$A_0 \Theta_{\text{in}}^2 \ll 1 , \tag{47}$$

eq. (43) becomes:

$$f_0 - x_{\text{in}} = A_0 y_{\text{in}} \Theta_{\text{in}} . \tag{48}$$

Inserting this into eq. (28) we obtain for the trajectory considered in section 5:

$$A_0 \Theta_{\text{in}} = A \int_{\Theta_{\text{out}}}^{\Theta_{\text{in}}} \mathrm{d}\theta \cos\theta \exp\{A(\cos\theta - \cos\Theta_{\text{in}})\} . \tag{49}$$

Requiring $\Theta_{\text{in}}^2 \ll 1$, $\Theta_{\text{out}}^2 \ll 1$, and using the parabolic approximation in the form (31):

$$A\Theta_{\text{in}}^2 \ll 1 , \qquad A\Theta_{\text{out}}^2 \ll 1 , \tag{50}$$

we have instead of eq. (49):

$$A_0 \Theta_{\text{in}} = A(\Theta_{\text{in}} - \Theta_{\text{out}}) ,$$

or:

$$\frac{A - A_0}{A} \Theta_{\text{in}} = \Theta_{\text{out}} . \tag{51}$$

Since $\Theta_{\text{out}}^2 \ll 1$, eq. (51) implies:

$$\left(\frac{A - A_0}{A}\right)^2 \Theta_{\text{in}}^2 \ll 1 . \tag{52}$$

This is the condition (34) discussed in section 5.

Refrences

1) S. van der Meer, CERN Report 61-7 (1961).
2) A. Ašner and Ch. Iselin, CERN Report 65-17 (1965) and CERN Report 66-24 (1966).
3) R. B. Palmer, Informal conference on *Experimental neutrino physics* (January 1965) CERN Report 65-32, p. 141 (1965).
4) V. L. Telegdi, Intern. Conf. on *Fundamental aspects of weak interaction* (Brookhaven 1963) BNL 837 (C-39), p. 170 (1963).
5) G. I. Budker, Intern. Conf. on *Accelerators* (Dubna 1963, Moscow) p. 282 (1964).
6) L. L. Danilov, S. N. Rodonov and G. I. Sil'vestrov, Sov. Phys. Techn. Phys. **12** (1967) 656.
7) V. I. Voronov, I. A. Danil'cenko, R. A. Rzajev and A. V. Samajlov, Internal Serpukhov Report IHEP 70-93 (1970).
8) H. Faissner, J. von Krogh and E. Fiorini, ECFA, 300 GeV Working Group, CERN/ECFA/72/4 vol. 1, p. 163 (1972).
9) H. Faissner, F. J. Hasert, J. von Krogh and W. Thomé, Aachen Report PITHA-59 (1972).